REVISTA MEXICANA DE CIENCIAS GEOLÓGICAS

Revista Mexicana de Ciencias Geológicas, v. 42, num. 3, December 2025, p. 145–159 ISSN-L 2007-2902 https://rmcg.unam.mx

Type: Original research



Lahars triggered by tropical storms at Volcán de Colima, Mexico: flow characteristics and morphological impact on the volcano slopes

Lucia Capra^{1,*}, Matteo Roverato², Gianluca Groppelli³, Víctor Hugo Márquez-Ramírez¹, Juan Carlos Gavilanes-Ruiz⁴, Raul Arambula-Mendoza⁵, Damiano Sarocchi⁶, Lorenzo Borselli⁶, and Roberto Sulpizio^{6,7}

¹ Instituto de Geociencias, Universidad Nacional Autónoma de México, UNAM-Campus Juriquilla, Blvd. Juriquilla 3001, 76230, Querétaro, Mexico.

² Dipartimento BIGEA, Alma mater Studiorum, Università di Bologna, Piazza di Porta San Donato 1, Italy.

³ Istituto per la Dinamica dei Processi Ambientali, Consiglio Nazionale delle Ricerche, Via Mangiagalli 34, 20133 Milano, Italy.

⁴ Facultad de Ciencias, Universidad de Colima, C. Bernal Díaz del Castillo 340, Villas San Sebastián, 28045 Colima, Colima, Mexico.

⁵ Centro Universitario de Estudios e Investigaciones de Vulcanología, Universidad de Colima, Bernal Díaz del Castillo #340, colonia Villas San Sebastián, 28045, Colima, Colima, Mexico.

⁶ Instituto de Geología, Universidad Autónoma de San Luis Potosí, Av. Dr. Manuel Nava 5, Zona Universitaria, 78240 San Luis Potosí, San Luis Potosí, Mexico.

⁷ Dipartimento di Scienze della Terra e Geoambientali, Università degli Studi di Bari Aldo Moro via Orabona 4, 70125, Bari, Italy.

EDITOR:Natalia Pardo Villaveces

How to cite:

Capra, L., Roverato, M., Groppelli, G., Márquez-Ramírez, V. H., Gavilanes-Ruiz, J. C., Arambula-Mendoza, R., Sarocchi, D., Borselli, L., & Sulpizio, R. (2025). Lahars triggered by tropical storms at Volcán de Colima, Mexico: flow characteristics and morphological impact on the volcano slopes. *Revista Mexicana de Ciencias Geológicas*, 42(3), 145–159 DOI: https://dx.doi.org/10.22201/iqc.20072902e.2025.3.1880

Manuscript received: May 31, 2025 Corrected manuscript received: September 16, 2025 Manuscript accepted: September 16, 2025 Published on line: December 1, 2025

COPYRIGHT

© 2025 The Author(s).

This is an open-access article published and distributed by the Universidad Nacional Autónoma de México under the terms of a Creative Commons Attribution 4.0 International License (CC BY) which permits unrestricted use, distribution, and reproduction in any medium, provided the original author and source are credited.





ABSTRACT

Rain-triggered lahars represent a frequent phenomenon at Volcán de Colima, Mexico. Hurricane Jova, on October 12th, 2011, was an anomalously rainfall event resulting in more than 240 mm of rainfall in 24 hours. This event triggered several lahars in the main ravines and induced multiple landslides on the valley sides. Based on data recorded at a seismic monitoring station along the Montegrande ravine, we were able to evaluate the lahar and obtain physical parameters of the flow and associated deposits. The lahar started around 7:20 a.m. (GTM) and lasted for approximately three hours. Five main flow pulses were detected. The first three pulses were closely spaced, and the final two occurred after one hour and 30 minutes, respectively. The event is classified here as a multi-pulse lahar, falling within the hyperconcentrated to debris flow regime. Three main depositional units were recognized along the ravine. The two lower units are up to 50 cm thick, massive, and mostly composed of sand and gravel. The upper unit is up to 1.5 m thick, massive with clasts embedded in a sandy matrix. The deep erosion observed along Montegrande ravine is related to the large magnitude (flow depth and velocity) of these flows, and to their long duration, with three hours of continuous scouring along the ravine. Immediately after the Jova event, dozens of landslides occurred along the ravine, some of which dammed the river and affected the flows during the 2012 lahar season. These landslides both initially trapped lahars and later provided debris for subsequent flow events, even during periods of low rainfall accumulation. The event here described is a clear example of large magnitude lahars at Volcán de Colima during tropical rainfall associated to hurricanes hitting the Mexican Pacific coast, as more recently occurred in 2015 with the transit of Hurricane Patricia. The findings of this study contribute to a better assessment of hazard scenarios in the case of extreme hydrometeorological events at Volcán de Colima and to understanding how their impact can drastically alter the hydrological balance of the volcano.

Keywords: Volcán de Colima; hurricane; tropical storm; lahar; debris flow; Mexico.

RESUMEN

Los lahares desencadenados por lluvias representan fenómenos muy comunes en el Volcán de Colima, México. El huracán Jova, el 12 de octubre de 2011, fue un evento de lluvia anómalamente significativo, que resultó en más de 240 mm de precipitación en 24 horas. Este evento desencadenó varios lahares en las principales barrancas e indujo múltiples deslizamientos de tierra. Con base en datos registrados en una estación de monitoreo sísmico ubicada a lo largo de la barranca Montegrande, fue posible registrar el lahar y obtener parámetros físicos del flujo y de los depósitos asociados. El lahar comenzó alrededor de las 7:20 a.m. (hora GMT) y duró aproximadamente tres horas. Se detectaron cinco pulsos principales de flujo. Los tres primeros ocurrieron con poca diferencia temporal entre ellos, mientras que los dos últimos se registraron tras una hora y 30 minutos, respectivamente. El evento se clasifica aquí como un lahar de pulsos múltiples, dentro del régimen de flujo hiperconcentrado a flujo de escombros. Se reconocieron tres unidades principales de depósito a lo largo de la barranca. Las dos unidades inferiores tienen hasta 50 cm de espesor, son masivas y están compuestas principalmente de arena y grava. La unidad superior tiene hasta 1.5 m de espesor, también masiva, con clastos embebidos en una matriz arenosa. La profunda erosión observada a lo largo de la barranca Montegrande está relacionada con la gran magnitud (profundidad y velocidad del flujo) del lahar, así como con su larga duración, con tres horas de erosión continua a lo largo de la barranca. Inmediatamente después del evento, ocurrieron decenas de deslizamientos de tierra a lo largo de la barranca, algunos de los cuales represaron el drenaje y afectaron el desplazamiento de los primeros lahares durante la temporada de lluvia del 2012. Estos deslizamientos obstruyeron el desarrollo de los primeros lahares y a su vez proporcionaron escombros para eventos de flujo subsiguientes, incluso durante periodos de baja acumulación de lluvia. El evento aquí descrito es un claro ejemplo de lahares de gran magnitud en el Volcán de Colima durante lluvias tropicales asociadas a huracanes que impactan la costa del Pacífico, como ocurrió más recientemente en 2015 con el paso del huracán Patricia. Los hallazgos de este estudio contribuyen a una mejor evaluación de los escenarios de riesgo en caso de eventos hidrometeorológicos extremos en el Volcán de Colima y a entender cómo su impacto puede alterar drásticamente el equilibrio hidrológico del volcán.

Palabras clave: Volcán de Colima; huracán; tormenta tropical; lahar; flujo de escombros; México.

INTRODUCTION

In recent years, hurricanes have caused catastrophic effects through their interaction with volcanoes worldwide. One recent example is the 2009 Hurricane Ida in El Salvador, which triggered landslides and debris flows from the Chichontepec volcano, resulting in 124 deaths. Another example is the 1998 Hurricane Mitch, which caused part of the inactive Casita volcano to collapse, producing a landslide that suddenly turned into a lahar, devastating several towns and killing 2000 people (Van Wyk Vries et al, 2000; Scott et al, 2005). A similar event occurred in 2005 when tropical storm Stan triggered landslides and debris flows from the Toliman Volcano (Guatemala), killing over 400 people in the Panabaj community (Sheridan et al., 2007). Other instances are found at volcanoes such as Pinatubo (Philippines), Merapi and Semeru (Indonesia), Soufrière (Montserrat), and Mt. Ruapehu (New Zealand), where tropical storms and heavy rainfall seasons often trigger large-scale lahars (Umbal and Rodolfo, 1996; Cronin et al., 1997; Lavigne et al., 2000; Lavigne and Thouret, 2002; Barclay et al., 2007; Dumaisnil et al., 2010; Doyle et al., 2010, de Bélizal et al., 2013).

Volcán de Colima (19°31'N, 103°37'W, 3860 m above sea level), one of Mexico's most active volcanoes, is periodically affected by intense seasonal rains that trigger lahars from June to late October (Davila *et al.*, 2007; Capra *et al.*, 2010; Capra *et al.*, 2018; Martínez-Valdes *et al.*, 2023). The most catastrophic event happened in 1955 when heavy rains caused several small landslides on the SW slope of Nevado de Colima, which combined to form a large debris flow in the Atenquique drainage, killing 23 people in the village of Atenquique and depositing 3.2 million cubic meters of debris (Saucedo *et al.*,

2008). Several hurricanes frequently hit the Pacific Coast each year but rarely reach inland to the Volcán de Colima region. The most recent notable hurricanes are Hurricane Patricia in 2015 and Hurricane Iova in 2011, the latter of which is the focus of this study. Hurricane Jova formed over the Pacific Ocean, made landfall along the Pacific coast on October 12th, 2011, as a Category 2 storm, and moved inland toward Volcán de Colima (Figure 1). It arrived as a tropical storm in the town of Coquimatlán, just 10 km southwest of Colima city, with winds up to 140 km/hr and 375 mm of rain over 24 hours. Manzanillo, one of the most vital commercial ports on the Pacific coast, along with other localities, was severely affected, and eight people lost their lives. Severe inland damage also occurred in Tecomán and Ciudad Armería due to flooding and sediment deposition by the Armería and Naranjo Rivers. Coquimatlán and Colima city experienced floods that damaged roads, bridges, and buildings, many requiring evacuations because of structural damage (https://www.excelsior.com.mx/2011/10/12/ nacional/774432). Landslides and sediment deposits from major rivers blocked the main interstate highway from Colima to Manzanillo and several smaller roads connecting Colima to villages on the western side of Volcán de Colima, leaving these areas isolated for several days.

The present paper aims to describe the hydro-meteorological response of the volcano during the Jova tropical rains, the characteristics of the lahar and related deposits, and the tremendous morphological changes in the Montegrande ravine that affected the lahars behavior during the subsequent 2012 rainy season, with important implications for hazard assessment. The example described here will contribute to a better understanding of such events, which regularly affect the Colima area, and to improving their hazard assessment.

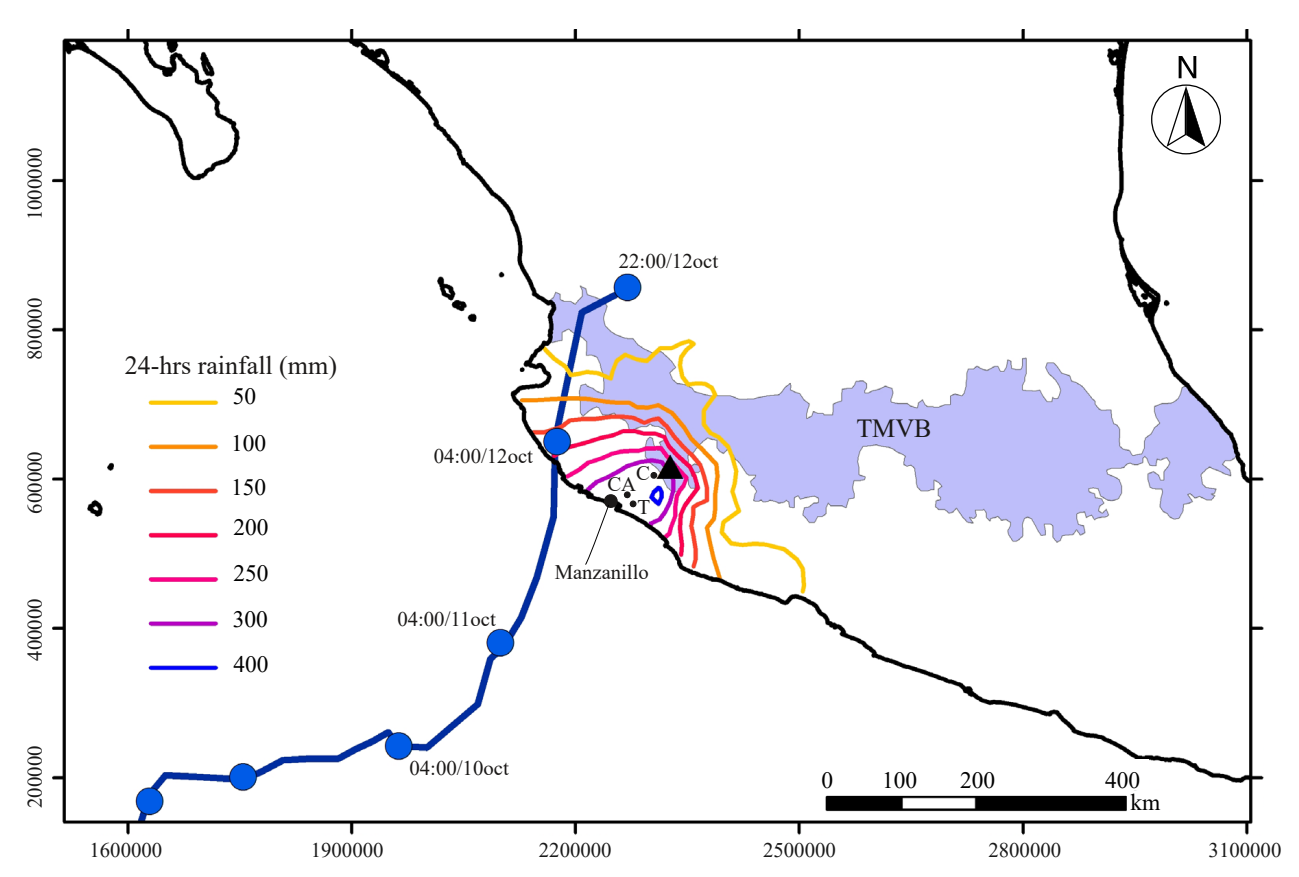


Figure 1. Sketch map of the Trans-Mexican Volcanic Belt (TMVB) where Volcan de Colima is located (black triangle), the trajectory of Hurricane Jova as it approached the Pacific coast and the total rainfall accumulation in the state of Colima. Abbreviations: C, Coquimatlán, CA, Ciudad Armeria; T, Tecomán.

LAHARS AT VOLCÁN DE COLIMA

Rain-triggered lahars are a common process during the rainy season (June-October) at Volcán de Colima (Davila et al., 2007; Capra et al., 2010). They typically affect areas up to 15 km from the summit, causing damage to bridges and power transmission towers. These lahars are more frequent immediately after eruptive events, such as dome collapses, which deposit block-and-ash flows—unconsolidated materials easily remobilized by water runoff during rain (Davila et al., 2007). Lahars are usually triggered by water runoff with enough entrainment to erode sediment from the riverbed. The critical stress needed to remobilize grains depends on the velocity and density of the slurry and the size of the grains in the streambed (Church & Jakob, 2020; Tang et al., 2020). Lateral erosion of the inner part of the channel also adds sediment to the flow. The source area of lahars at Volcán de Colima includes the uppermost unvegetated zone, with slopes ranging from 40° to 20°, decreasing to 10° at 5 km from the crater, where vegetation densely covers older terraces composed of debris avalanches and pyroclastic deposits from past eruptions. Five major watershed areas, ranging from 1 to 4 km², feed the main ravines (Capra et al., 2010; Capra et al., 2018). According to real-time monitoring, lahars consist of a sequence of surges, each with a block-rich front followed by a main body and a recessional tail (Vázquez et al., 2014, 2016a). Flow types range from debris flows (>60 % vol) to hyperconcentrated flows (20-60% vol of sediments), and their magnitude and sediment content are mainly determined by the total rainfall accumulation (Capra et al., 2018).

At Volcán de Colima, at the beginning of the rainy season (June-July), rainfalls are characterized by high peak intensities around 100 mm/h but with short durations of less than an hour; total

accumulated rainfall during such events is usually only 20–30 mm (Capra *et al.*, 2010). Late in the rainy season, tropical rainfall can last several hours, with more than 100 mm of accumulated rainfall, but at a lower intensity of ~ 50 mm/h. These two different types of meteorological events can both trigger lahars, but they generate flows with distinct characteristics. High peak-intensity rainfalls at the beginning of the rainy season typically trigger lahars (with or without antecedent rain), producing single-pulse flows, in response to the hydrophobic characteristics of volcanic soils under dry soil conditions (Capra *et al.*, 2010). In contrast, late in the rainy season, when soil maintains very humid conditions, hurricane-related storms trigger lahars only after significant antecedent rainfall has accumulated, and they generate multiple-pulse flows whose time sequence is related to the watershed peak discharge (Capra *et al.*, 2018; Coviello *et al.*, 2018; Capra & Caballero, 2021).

LAHAR MONITORING AT VOLCÁN DE COLIMA

In 2007, a monitoring program was launched at Volcán de Colima. Initially, only two rain gauges were installed (A and MG-N sites, Figure 2a), and lahar events were detected by the seismic network of RESCO, the seismological network of Colima University, which is primarily dedicated to monitoring volcanic activity and is widely distributed (Davila *et al.*, 2007; Zobin *et al.*, 2009; Capra *et al.*, 2010). In 2011, a better-equipped station was established at the Montegrande ravine (MG-M site, Figures 2a and 2b), but it was eventually destroyed by pyroclastic density currents during the 2015 eruption (Capra *et al.*, 2016). This station consisted of a 12-meter-high tower with a

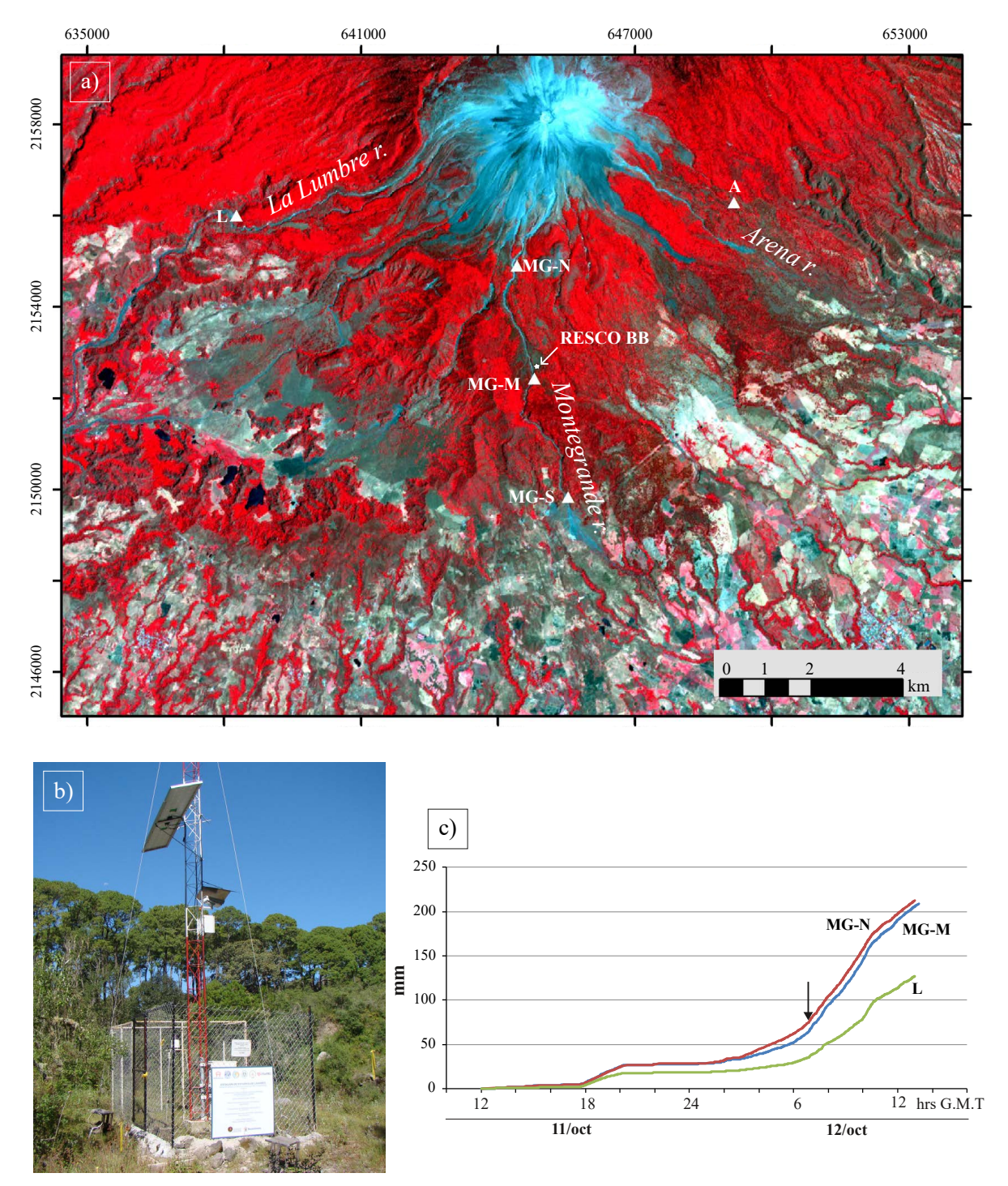


Figure 2. a) Aster image (4, 5 and 7 bands in RGB combination) showing the location of the monitoring sites in 2011 on the southern sector of the volcano. At La Arena site (A) a rain gauge was installed in 2007; in 2011 the Montegrande ravine was the most monitored, with a rain gauge sensor at site MG-N and a real-time monitoring system (MG-M site), including videocamera, rain and soil moisture sensors, a broadband seismic station and a geophone; at the end of the ravine, a second geophone was installed (MG-S site). The RESCO broadband station (Resco BB) was 500 NE of this site. b) Photograph of the MG-M monitoring site. c) Rainfall measured at the rain gauge stations installed on the volcano slope.

directional antenna transmitting data in real time to RESCO facilities, a camera, a station equipped with a rain gauge paired with a soil moisture sensor, and a 10 Hz geophone that logs data on a mini SD card. A second 10 Hz geophone was also installed at the end of the Montegrande ravine (MG-S, Figure 2a). The camera continuously recorded images every two seconds, with a resolution of 704×480

pixels. The rain gauge (HOBO RG3) recorded rain accumulation at one-minute intervals, as did the soil moisture sensor (HOBO EC10), which was installed 10 cm below ground level. A 3-component Guralp CMG-6TD broadband seismometer, part of the RESCO seismic network and installed 500 meters northeast of the MG-M site, recorded data at a sampling rate of 100 Hz (RESCO-BB, Figure 2a).

METHODS

Seismic data were obtained from the vertical component of the seismogram recorded by the broadband station (RESCO BB, Figure 2a). The spectrogram was generated using the Fast Fourier Transform (FFT) with a 10-second window and 50% overlap, while the Real-Time Seismic Energy Measurements (RSEM) were calculated using a 60-second window.

At the monitoring site, topographic profiles were obtained during various field campaigns using a Leica DistoX3 laser distance meter.

Grain-size studies were conducted using three different analytical methods to encompass the entire grain size spectrum. Fine sand to clay particles (4 to 9 phi) were studied using a photosedimentograph, while medium sands to coarse pebbles (5 to -4 phi) were analyzed by mechanical sieving. Coarser fragments were analyzed using optical methods. The optical method used was the Rosiwal intercept method, which provides stereologically correct volumetric data from a scaled photograph (Sarocchi *et al.*, 2011). Statistical parameters were obtained using the DECOLOG 4.0 program (https://www.lorenzo-borselli.eu/decolog).

RESULTS

The Hurricane Jova: total rainfall and hydrological characteristics of the source area

Figure 1a shows the trajectory and rain distribution for Hurricane Jova as reported by the National Weather Service based on rain gauge records at Coquimatlán, Colima, and Manzanillo. The maximum rain accumulated in the region was around 300 mm over 24 h. The three stations installed on the volcano slopes recorded similar rainfall amounts with a maximum value of 204 mm registered at both stations along the Montegrande ravine (Figure 2c), with maximum peak intensity of 42 mm/h (calculated in a constant time step of 5 minutes). Rainfalls associated with Hurricane Jova were similar to those of typical late-season hurricane-related tropical storm events, characterized by a low peak intensity of 50–60 mm/h, but with total rainfall accumulation exceeding 100 mm over several hours (Capra et al., 2018).

The Jova lahar: flow characteristics

Based on the RESCO-BB seismic record, the lahar began early in the morning of October 12th, 2011 (Figure 3a). From now on, we will refer to the event as the Jova lahar. The seismic signal shows the typical waveform of lahars, characterized by a long-lasting record with several peaks in amplitude and the highest energy in frequency content, interpreted as pulses or surges (Doyle et al., 2010; Vázquez et al., 2016a). The event started around 7:20 a.m. GMT after about 60 mm of rain had accumulated (Figure 3b). The seismic amplitude displays three main wave packages. The first package (I) features three closely spaced pulses that lasted about an hour. After roughly one hour, a single, distinct pulse (II) appears, followed 30 minutes later by the largest and most energetic wave package, reaching a maximum amplitude of 0.4 mm/s, accompanied by a "train" of seismic peaks that persisted for over an hour. The geophone at the MG-M site (Figure 3c) recorded three main packages as well, with the signal saturating during the third. The distal geophone (MG-S) experienced saturation from the first arrival, showing a continuous discharge for nearly 3-4 hours (Figure 3c).

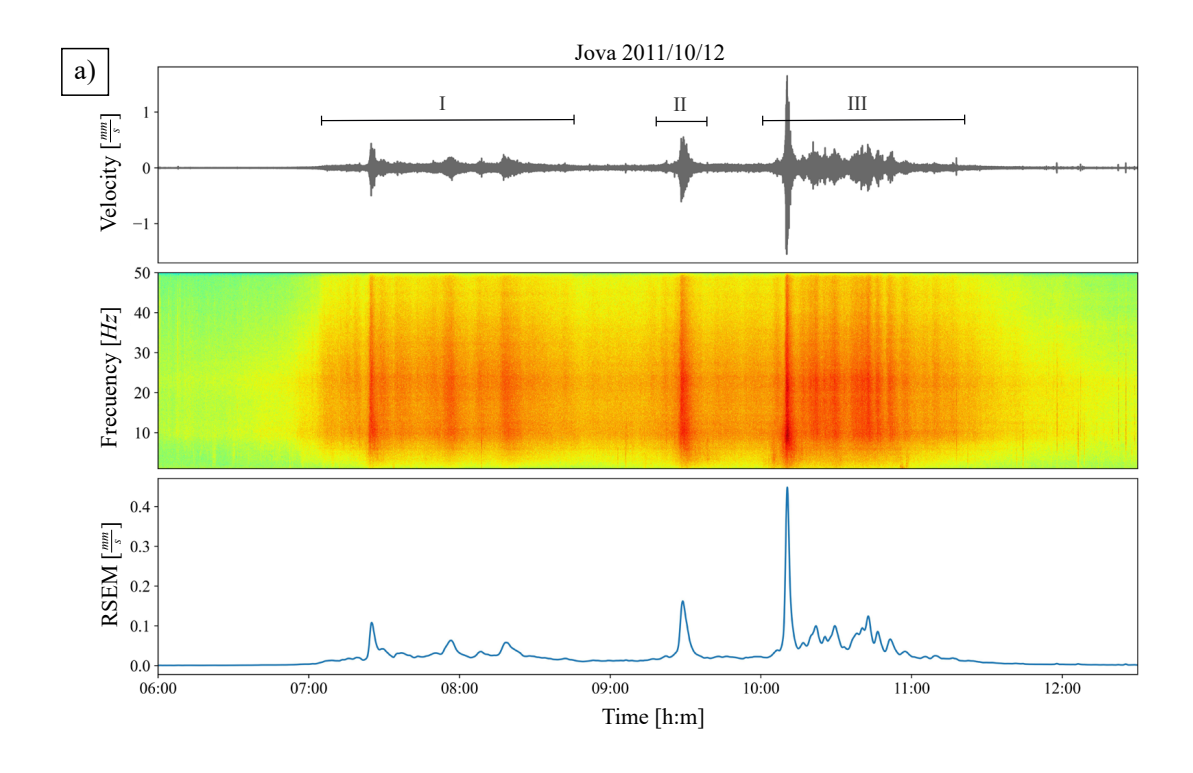
Since the Jova lahar occurred overnight, no images of the event are available. The flow characteristics were determined by comparing images of the monitoring site taken before and after the event, along with indirect evidence collected during fieldwork conducted three days later. By examining the photos taken at the monitoring point, it is clear that the lahar was highly erosive at this location. The main terrace was eroded by at least 1 m in width and up to 2 m in depth (Figures 4a, 4b, and 4f). Flow marks on trees and the inundation limits on older terraces indicate maximum flow depths of approximately 4 m in the middle reach and 2 m in a more distal part of the ravine, with crosssectional wetted areas of 15-20 m² (Figure 5). Estimating an average depth along the channel is difficult because the ravine's width rapidly varies downstream, from 3 m to 15 m (Figures 5c and 5d). Additionally, the high-water marks observed could be related to different pulses or to a different pre-erosion or pre-accumulation substratum level. Despite this, the flow peak discharge at the monitoring site is estimated to be about 150 m³/s, based on the inundated cross-sectional area and a maximum flow velocity of 8-10 m/s, calculated using the superelevation method near the monitoring point. As demonstrated in previous studies (Cole et al., 2009; Caballero & Capra, 2014; Martínez-Valdés et al., 2023, Márquez-Ramirez et al., 2025), seismic amplitude can define the flow hydrograph; considering the estimated maximum flow discharge (i.e., maximum seismic amplitude) from the envelope of the seismic signal (Figure 3a), a conservative volume of 200000 m³ is estimated (Figure 6).

Characteristics of the deposit

Fieldwork was carried out three days after the event, and three main depositional units were identified, extending up to 15 km from the summit area (Figure 7). These units create overlapping terraces in the middle part of the channel and clast-rich lateral levees on older terraces. The primary depositional unit appears in the middle reach, is up to 1.5 m thick (unit B, Monte 32, 19 and 17, 12 and 9, Figure 7), and consists of massive, matrix-supported, ungraded or normally graded deposits, with clasts up to 15 cm in diameter embedded in a sandy matrix (e.g., Monte 17 section in Figure 8a). This unit is also associated with numerous logs, observed as overbank deposits on older terraces. Most logs are aligned parallel or perpendicular to the flow direction, as seen in an overbank bend area of the river (Figure 9). Toward the top, the deposit gradually shifts to a more dilute, massive, sandy layer (sections Monte 32 and 17, Figures 7 and 8a). Unit B overlies two layers (Unit A), which are up to 50 cm thick, massive, and composed of sandy gravel (sections Monte 12 and 9, Figure 7). The outcrops of these basal units are quite discontinuous, making downstream correlation difficult. Where the ravine opens onto the distal depositional fan (Figure 5e and 5f), the sequence includes less than 0.5-m-thick, massive, sandy layers (Unit C), some showing weak stratification (Monte 47 and Monte 40, Figure 7). An interesting feature observed at pinch points along the ravine is the presence of large boulders lodged where the channel narrows to less than 3 m. These jammed boulders formed small barriers (~1 m high) that promoted sediment buildup behind them.

The grain-size analyses of the deposits show a very low percentage of silt fraction (<10 wt%, Table 1) with no clay in all collected samples. Unit B is dominated by gravel (up to 66 wt%) and can exhibit normal grading with a gradual decrease in grain size toward the top (Figure 8a). Unit A displays a predominance of sand, ranging from 50 to 80 wt% of the entire deposit (Figure 8b). Distal deposits (Unit C) are finer than those in the middle reach, containing less than 10 wt% gravel (Figure 8b), and are better sorted (Table 1). No samples were collected in the proximal reach (0–3.5 km) because no fresh outcrops were observed; instead, only erosive surfaces associated with the transit of the lahars were found.

In summary, by combining textural and granulometric characteristics, the lahars emplaced debris-flow deposits in the middle



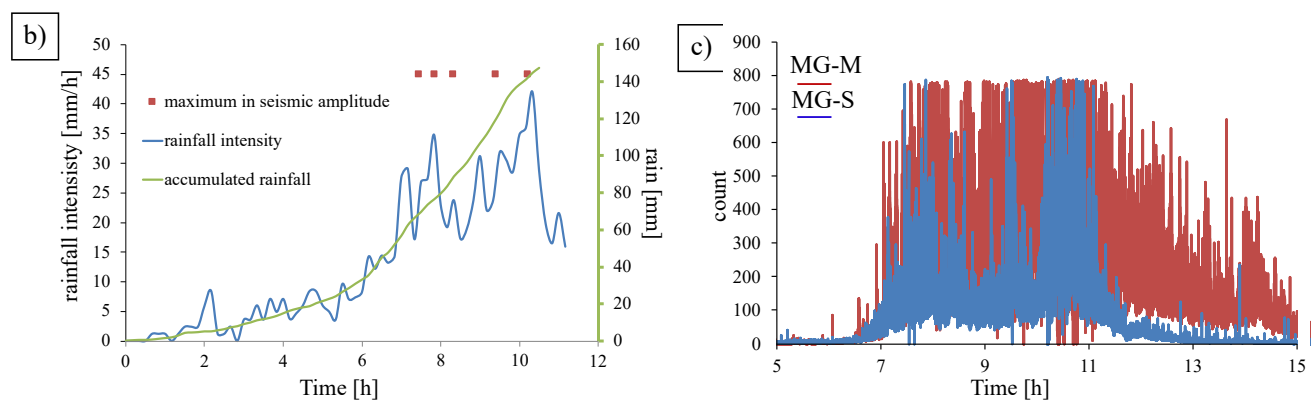


Figure 3. a) Seismic record of the October 12th, 2011 event (seismogram, spectrogram and RSEM curve) from RESCO-BB station; three main seismic wave packages are indicated; b) accumulated rainfall and intensity at the MG-M site; squares indicate the start of the detected seismic peaks; c) Geophone signal at MG-M and MG-S sites.

reach and more common hyperconcentrated flow deposits in the distal reach (Figure 8b).

Rainfall-induced landslides: morphological modification of Montegrande ravine and effect on the 2012 lahar season

The lower flanks of the Volcán de Colima are primarily made up of unconsolidated debris-avalanche deposits interlayered with pyroclastic-flow and secondary debris-flow successions (Cortes *et al.*, 2005, 2010; Roverato *et al.*, 2011). Major ravines have carved into this material, and vertical walls of these volcaniclastic successions line the roads. The heavy rains from Hurricane Jova caused soil slides and rock flows (terminology based on Hutchinson, 1988) that remobilized masses of a few thousand cubic meters, blocking main roads and isolating some communities for days. Similar events were observed along Montegrande ravine (Figure 10). Field evidence suggests that most landslides occurred after the Jova lahar. A week later, we mapped several landslides along the ravine (Figure 10a), which varied greatly in size. These landslides completely blocked the river channel with

thicknesses reaching up to 10 m (Figures 10b, 10c, and 10d). We identified 61 landslides, with 60% situated along the bends and the rest along the straight sections. With few exceptions (nine cases), landslides were located where the ravine wall slope exceeds 20° , often more than 40° . Based on measurements of maximum thickness and the extent of each mass blocking the channel, we estimated the average volume for each landslide. Values ranged from a maximum of $1000 \, \text{m}^3$ to a minimum of $20 \, \text{m}^3$, with most falling within tens to hundreds of cubic meters. The total combined volume of these landslides was approximately $70000 \, \text{to} \, 100000 \, \text{m}^3$.

The Jova lahar was the last event recorded during the 2011 rainy season, and these landslide deposits acted as small natural dams, controlling flow behavior during the 2012 rainy season. The first detected lahar in 2012, on June 25th, clearly shows evidence of this phenomenon. The seismic record of RESCO-BB shows a main pulse that lasted less than five minutes, followed by two other minor seismic peaks (Figure 11a). Based on our rain gauge at MG-M site, this lahar was associated with only approximately 25 mm of rain accumulated

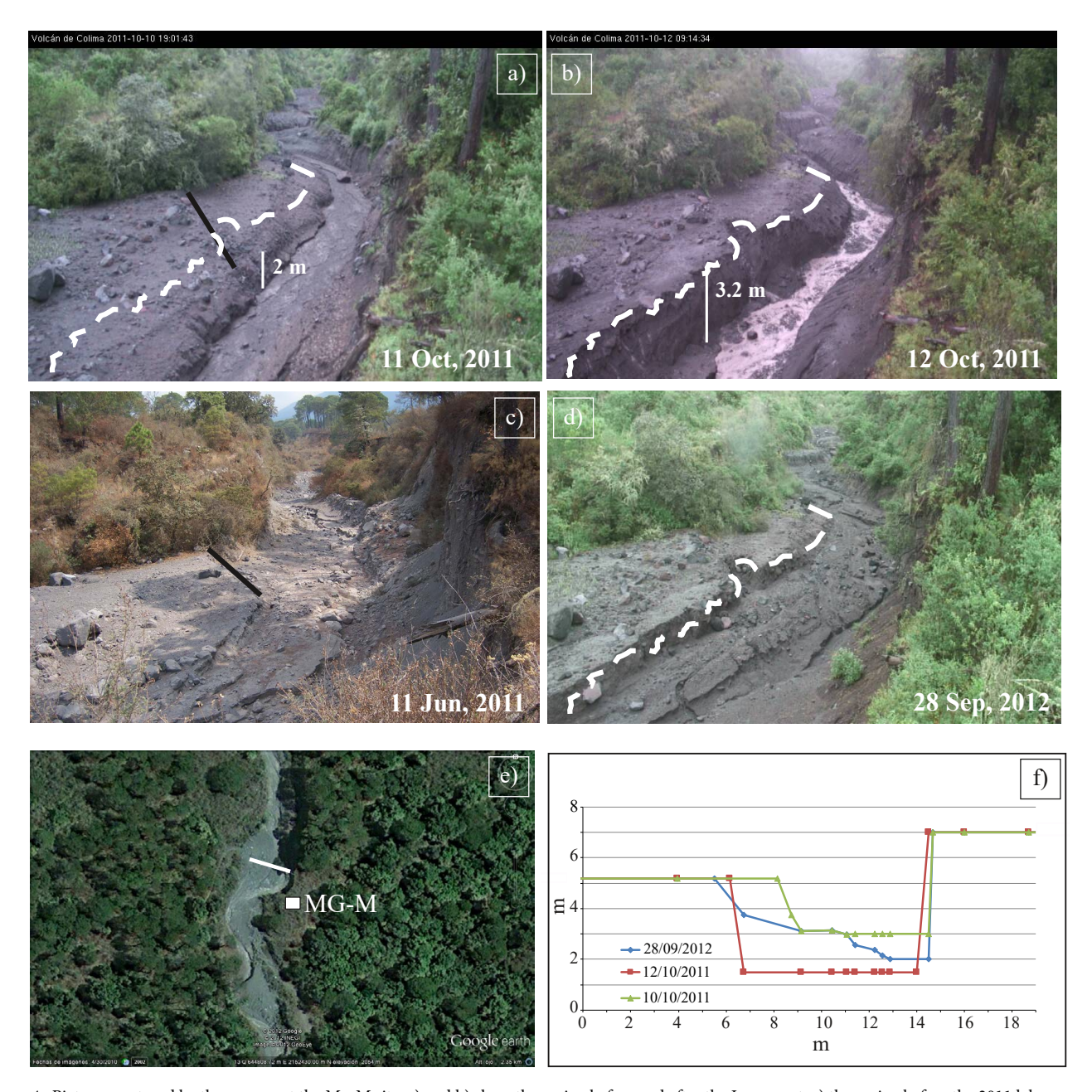


Figure 4 . Pictures captured by the camera at the Mg-M site, a) and b) show the ravine before and after the Jova event; c) the ravine before the 2011 lahar season and, d) towards the end of the 2012 rainy season; e) Google Earth image showing the trace of the topographic profiles of figure f).

in about one hour (Figure 11b). A video taken by a person standing at the side of the channel, a few meters downstream of the MG-M site, captured the lahar as it overflowed a mass that was obstructing the channel, slowed down, and partially ponded behind this barrier (Figure 12). The event consists of a fully developed flow with a block-rich front (Figure 12b) followed by a body that overflowed the obstruction (Figure 12c). We could not determine if this obstruction was fully eroded by the end of the event (which lasted around 30 minutes). However, we infer that the flow was trapped downstream by a larger obstruction since the signal detected by the geophone at the end of the ravine (MG-S) was very weak, similar to background noise (Figure 11b). The next day, on June 26th, a new event was recorded, but, as observed the day before, the downstream geophone only detected background noise, again indicating that at some point

the lahar had been trapped. It was only on June 29th that the distal geophone recorded a strong signal typical of a well-developed lahar. During a field survey on September 20th, 2012, we noted that all the obstructions had already been eroded in the central portion of the channel (Figures 9e, 9f and 12d). At the MG-M site, the channel bed was between 1 and 2 m higher than the bed level at the time of Hurricane Jova (Figures 4b and 4d).

DISCUSSION

The intense rainfall that affected Volcán de Colima during the passage of Hurricane Jova had severe effects on the area, particularly along the main ravines. At that time, a lahar monitoring system was



Figure 5. Photographs taken along the Montegrande ravine three days after the Jova lahar with evidence of flow depth (white line). a) Gravel and sandy patches on top of large boulder, b) erosive surfaces and small landslide, c) overbank deposits. Photos d), e) and f) show the change in width of the channel in the distal area. The location of each site is indicated in Figure 7.

available only at the Montegrande ravines, based on which we were able to realize a comprehensive analysis of the event and the associated morphodynamic effects, providing essential information about lahar behavior at Volcán de Colima.

Based on the seismic record and its features, the Jova lahar is described as a multiple-pulse event (Vazquez *et al.*, 2016a), characterized by a series of main surges that show a good timing connection with the highest peak rainfall intensities (Figure 3b). Rainfall-runoff models link this quick response to the elongated

shape of the watershed feeding the Montegrande ravine (Capra et al., 2018). The initial pulses are hyperconcentrated flows (wave packages I and II, Figure 3a) that come before the main block-rich debris flow, which progressively dilute into a turbulent hyperconcentrated tail (wave package III). The entire event lasted over three hours, with varying time gaps between pulses (up to an hour), during which dilute, sediment-loaded water flowed over the riverbed. The textural and granulometric features of the deposits also reflect this sequence of events, with massive, laminated layers at the bottom (Unit A),

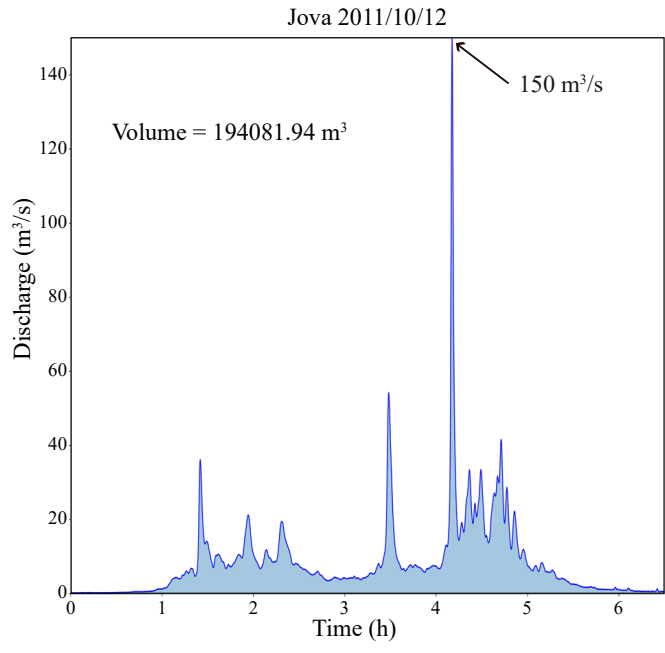


Figure 6. Flow discharge curve obtained from the envelope of the seismic amplitude (Figure 5a) and considering a maximum flow discharge of 150 m³/s. The area below the curve corresponds to the volume of the flow passing through the MG-M monitoring site.

covered by the main debris flow deposit that transformed to a more dilute, hyperconcentrated flow deposit (Unit B). Changes in grain size toward the upper part of the unit (Figure 8a) align with the changes in flow discharge seen in the seismic signal (wave package III, Figure 3a). A gradual change in grain size is also visible toward the distal reach (Unit C, Figure 8b), which is typical of lahars that become more diluted downflow (Thouret et al., 2019). Finally, the main flow pulse transported and deposited logs on top of lateral terraces, with their orientation suggesting a laminar flow during the peak flow stage (Figure 9). The block-rich fronts seem to be a common feature of large lahars at Volcán de Colima (Vazquez et al., 2016a; Márquez-Ramirez et al., 2025), made up of massive, turbulent boulder dams filled with a slurry matrix, usually triggered by either large or small intense rainstorms (Okano et al., 2012).

Channel erosion during lahars occurs both during the transit of the main debris-flow body, which exerts high pressure and shear stress on the base and walls of the channel, and during hyperconcentrated flows through turbulence (Fagents & Baloga, *et al.*, 2006; Doyle *et al.*, 2011). During the Jova episode, deep (up to 4 m), high-velocity (10 m/s), and long-lasting (up to three hours) flows affected the Montegrande ravine, promoting its erosion as observed at the monitoring site (Figure 4) and indirectly from the numerous landslides triggered after the event (Figure 5), likely enhanced by basal erosion (undermining) at the bases of the channel walls caused by the flow, which may also have transmitted ground vibrations through partially water-saturated slopes. Based on the data presented here, it is clear that

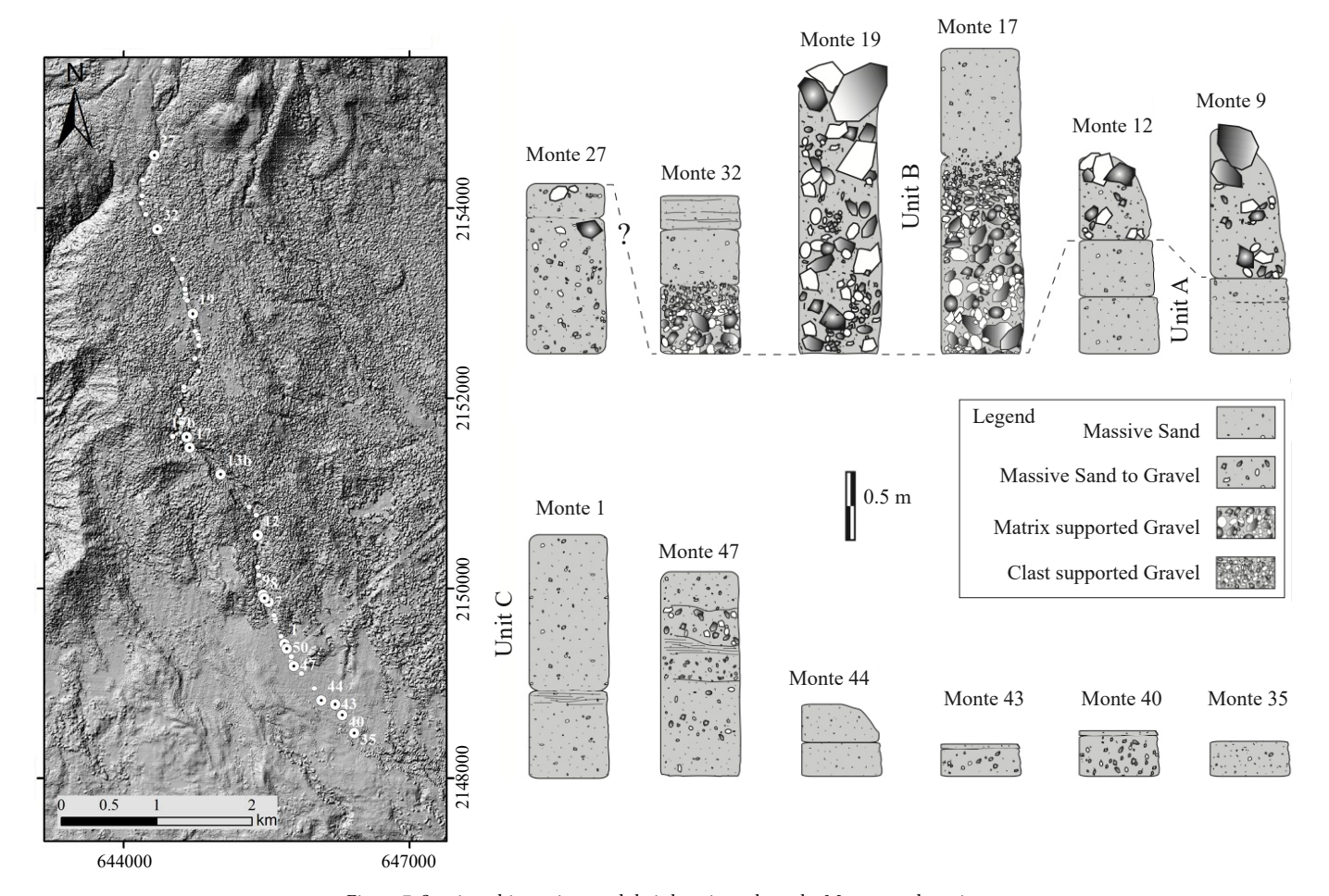


Figure 7. Stratigraphic sections and their locations along the Montegrande ravine.

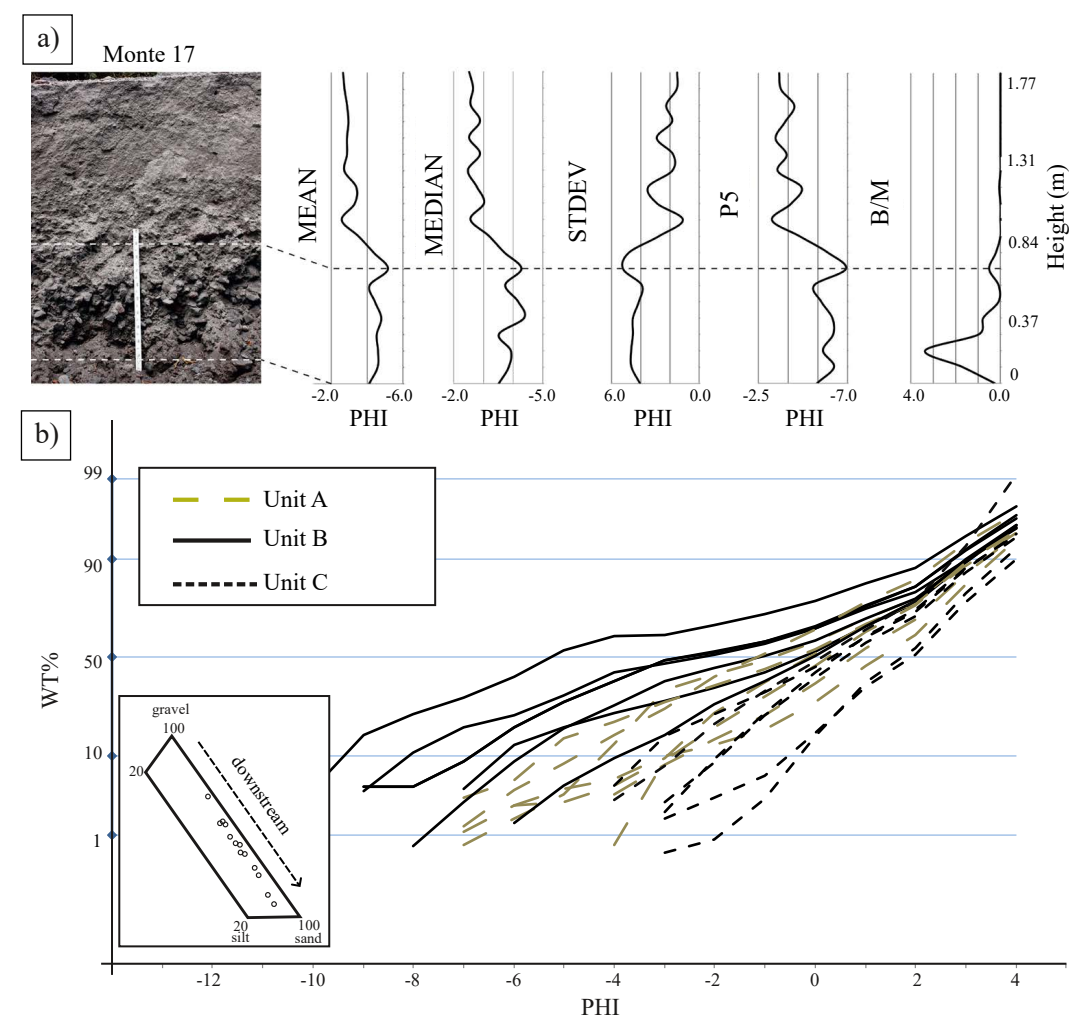


Figure 8. a) Vertical granulometric profiles of section Monte 17, where normal grading is easily recognizable. This profile was performed using Rosiwal method over digital image of the outcrops. Abbreviations are: STDEV: Standard Deviation; P5: percentile 5%; B/M: blocks vs. matrix. b) Cumulative curves of analyzed samples, showing a general decrease in grain size of samples downflow. The inset depicts the low silt content for all samples and a general decrease in grainsize downstream.

lahars at Volcán de Colima control the morphological evolution of the volcano ravines, regardless of whether ongoing magmatic activity is present. Even if lahars are more frequent immediately after an eruptive phase (Davila et al., 2007), meteorological events determine the magnitude and duration of the flow (Capra et al., 2010, 2018; Martinez-Valdes et al., 2023). As previously noted (Capra et al., 2010), low-volume lahars (10⁴–10⁵ m³) typically develop during short-lived (<1 h), high-intensity (>80-100 mm/h) orographic rainstorms at the onset of the rainy season, and they dissipate rapidly once rainfall ceases (Vázquez et al., 2014, 2016a). In contrast, large-volume lahars (10⁵-10⁶ m³) with multiple flow pulses occur during prolonged (>2-48 h), low-intensity (~50 mm/h) rainfall events, such as tropical storms (Capra et al., 2010, 2018; Martínez-Valdes et al., 2023). Figure 4a shows a picture of the ravine at the monitoring site, on the day before the Jova lahar, where the channel was 2 m deep (Figure 4a and 4f); the Jova lahar drastically eroded the channel, making it deeper and wider (Figure 4b). During the 2012 lahar season, no large events were detected. Instead, the channel gradually filled with sediment deposited by smaller lahars (Figure 4d, 4f, and 10f), a process further enhanced by several landslides that obstructed the main channel, particularly at the onset of the rainy season. These observations align with previous findings. Vázquez et al. (2016b) observed that lahars thicker than 2 m can exert a basal shear stress sufficient to erode the streambed. Small lahars thus promote the morphological recovery of the volcano slope through downstream aggradation that induces the rise of the channel bed by slope decrease, as well as accumulation of pebbles on its surface, all factors promoting a depositional regime. Under these conditions, only deep flows with high basal shear stress can erode the substratum (Gran & Montgomery, 2005). This recovery process appears common during inter-eruptive phases of active volcanoes, when sediment yields return to pre-eruption levels (Manville *et al.*, 2009). However, at Volcán de Colima, this recovery process is interrupted by intense rainfall events that generally occur once a year, at the end of the rainy season when tropical storms are common (Capra *et al.*, 2010; 2018), triggering multiple-pulse, highly erosive lahars, after which a new cycle of morphological recovery may begin.

CONCLUSIONS

The 2011 Hurricane Jova triggered a lahar 200000 m³ in volume, which caused intense modification of the Montegrande ravine, including deep erosion and subsequent shallow landslides along the channel. After Jova, hurricanes Manuel (2013) and Patricia (2015)

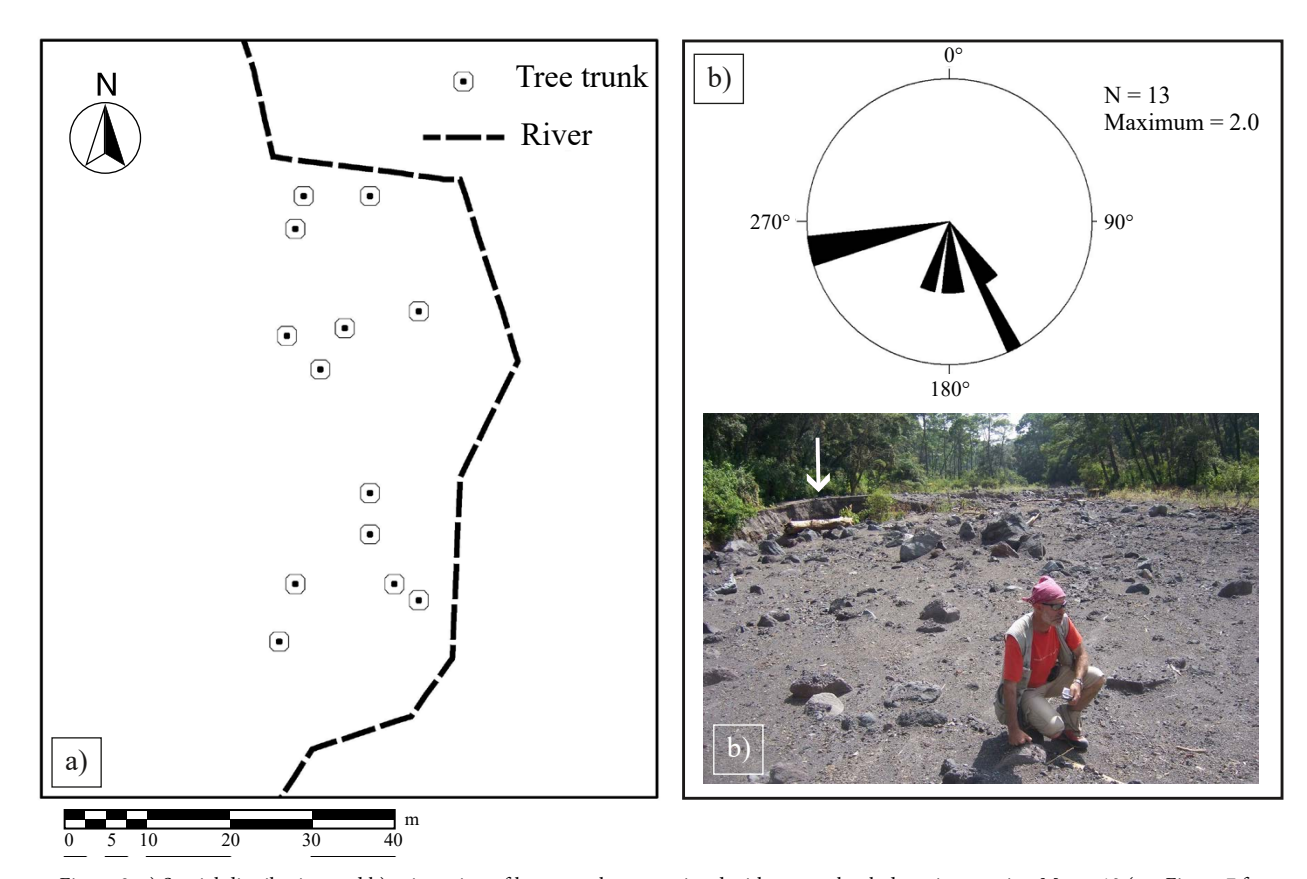


Figure 9. a) Spatial distribution and b) orientation of large tree logs associated with an overbank deposit at section Monte 12 (see Figure 7 for location). c) Panoramic view of the terrace at section Monte 12.

 ${\it Table 1. Granulometric \ parameters \ of \ analyzed \ sections.}$

Sample	Gravel wt%	Sand wt%	Silt wt%	Mean Md (phi)	Std dev $\sigma_{I}(phi)$	Skewness Sk ₁	Kurtosis K
Montela	40.93	54.47	4.59	-0.72	2.87	0.08	0.68
Monte 1b	12.52	81.36	6.12	1.04	2.39	-0.25	1.26
Monte 1c	34.79	60.96	4.26	-1.03	3.61	-0.26	0.79
Monte7	51.29	45.53	3.19	-2.46	4.26	-0.06	0.76
Monte9	23.38	72.01	4.62	-0.01	2.42	0.05	0.86
Monte12a	52.42	42.98	4.60	-2.14	3.91	0.15	0.74
Monte12b	52.91	43.60	3.48	-2.23	3.82	0.13	0.75
Monte12c	35.84	58.91	5.25	-0.85	3.38	-0.16	0.80
Monte17a	44.43	51.07	4.50	-1.26	3.50	-0.05	0.73
Monte19	66.46	31.10	2.44	-4.35	4.52	0.28	0.73
Monte 20	7.45	86.26	6.30	1.10	2.05	-0.08	1.07
Monte27	39.78	57.20	3.02	-1.04	2.86	0.02	0.98
Monte32a	27.11	68.75	4.15	-0.17	2.68	-0.09	0.90
Monte 32b	18.00	77.14	4.86	0.20	2.28	0.00	0.87
Monte 32c	14.04	80.48	5.48	0.59	2.31	-0.10	1.02
Monte44	3.32	86.78	9.90	1.80	1.76	-0.11	0.99
Monte44b	0.89	91.44	7.67	1.69	1.56	0.00	0.90
Monte35	9.09	85.34	5.58	0.53	2.02	0.12	0.89
Monte46	8.53	85.60	5.87	0.65	2.05	0.07	0.88
Monte40	19.26	79.91	0.83	0.10	2.18	-0.06	0.80
Monte51	23.08	71.53	5.39	0.04	2.62	-0.11	0.83

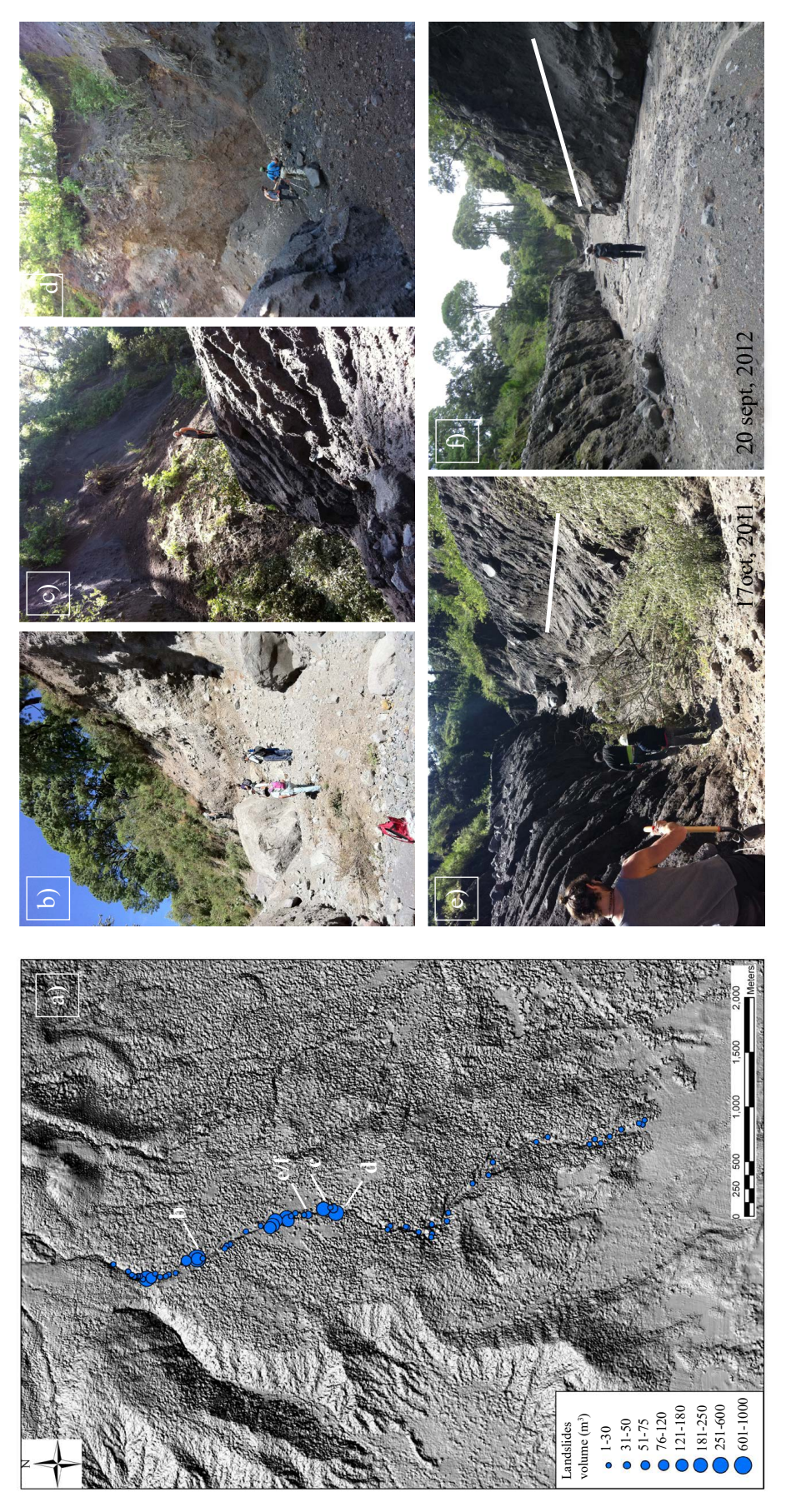


Figure 10 . a) Shaded relief showing the sites where landslides were identified. The dot size is proportional to the estimated volume of each landslide. Letters correspond with those used to identify pictures. (b), (c) and (d) are large landslide bodies that completely blocked the channel, with maximum height of 10 m. (e) and (f) show the same site before and after the 2012 lahar season. Note as lahars removed the channel obstruction and raised the channel floor (the white line marks the same reference position in both images).

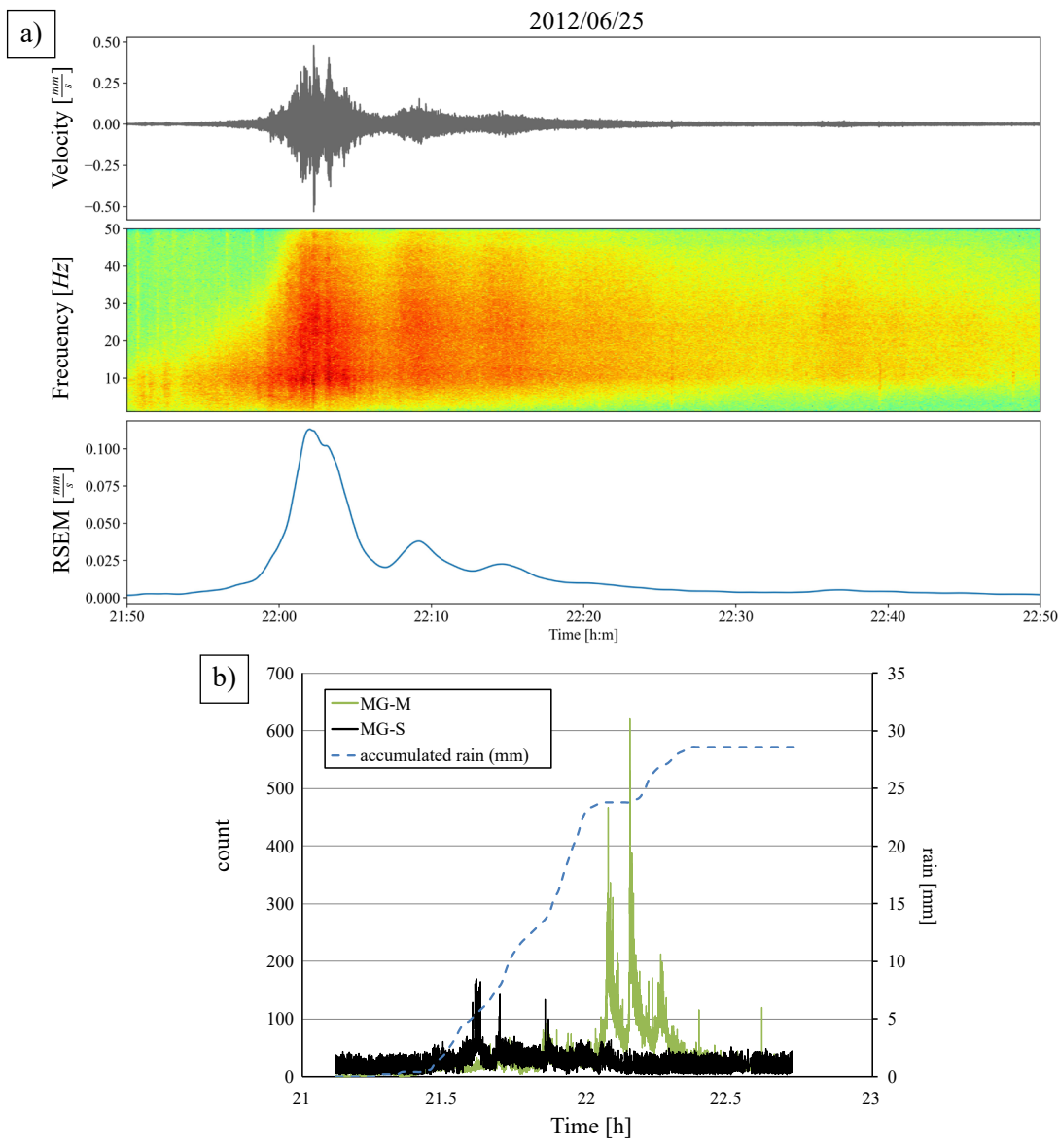


Figure 11. a) Seismic record of the June 25th, 2012 event (seismogram, spectrogram and RSEM); b) geophone signals at MG-M and MG-S sites with the total accumulated rain.

also had similar catastrophic effects on the area (Capra *et al.*, 2018; Martinez-Valdés *et al.*, 2023). These meteorological events represent exceptional episodes that can threaten towns within a 15 km radius of the volcano summit, including the interstate road between the states of Colima and Jalisco. If a hurricane is forecasted to reach the coast of Colima, mitigation measures can be implemented near bridges through sediment removal and the construction of earthen dikes along the channels that cross populated areas. These measures can help limit damage to infrastructure and prevent loss of life.

Acknowledgements. This work was supported by CONACyT 99486, PAPIIT-UNAM IN-106710, SRE-CONACYT 146324 projects to Lucia Capra. The Ministry of Foreign Affairs of Italy and SRE of Mexico provided travel assistance to Gianluca Groppelli. Roberto Sulpizio acknowledges the short mobility program of CNR of Italy. Thanks to José Luis Ortiz and Sergio Rodríguez, from the Centro de Prevención de Desastres (CENAPRED), who in 2011 established the instrumentation at the Montegrande monitoring site.

Author contributions. LC: Methodology, investigation, data processing, analysis and interpretation, writing, review, editing, and resource management. MR, GG, DS, LB, RS: Investigation, methodology, interpretation and review. VHMR, JCGR and RAM: Investigation, data processing, interpretation. All authors discussed the results and contributed to the writing of the manuscript.

Data avaliability statement. The authors declare that the data supporting the findings of this study are available upon request from LC. **Declaration of Competing Interests.** The authors declare that they are not aware of any financial conflicts of interest or personal relationships that could have influenced the work reported in this article. LC served as associate editor of the Revista Mexicana de Ciencias Geológicas during the time this manuscript was reviewed and accepted, and having had no involvement in the peer review or editorial decisions regarding this manuscript.

Funding. This work was supported by CONACyT 99486, PAPIIT-UNAM IN-106710, SRE-CONACYT 146324 projects to Lucia Capra. The Ministry of Foreign Affairs of Italy and SRE of Mexico provided



Figure 12. Still image showing the Montegrande ravine prior (a) and during the arrival of the block-rich front of June 25, 2012, lahar. The front of the flow is characterized by a boulder-dam with interstices filled with slurry matrix; c) Photo showing the lahar overflowing the obstruction and d) after the obstruction was eroded entirely.

travel assistance to Gianluca Groppelli. Roberto Sulpizio acknowledges the short mobility program of CNR of Italy.

REFERENCES

- Barclay, J., Alexander, J., & Susnik, L. (2007). Rainfall-induced lahars in the Belham valley, Monserrat, Wst Indies. *Journal of the Geological Society* of London, 164(4), 815–827. https://doi.org/10.1144/0016-76492006-078
- Caballero, L., & Capra, L. (2014). The use of FLO2D numerical code in lahar hazard evaluation at Popocatépetl volcano: a 2001 lahar scenario. Natural Hazards and Earth System Sciences, 14(12), 3345–3355. https:// doi.org/10.5194/nhess-14-3345-2014
- Capra, L., & Caballero, L. (2021) Rainfall on active volcanoes: morphological response and associated processes. In J. R. Comino (ed.) Precipitation: Earth Surface Responses and Processes (pp. 327–347). Elsevier. https://doi.org/10.1016/B978-0-12-822699-5.00012-4
- Capra, L., Borselli, L., Varley, N., Norini, G., Gavilanes-Ruiz, J. C., Sarocchi, D., & Caballero, L. (2010). Rainfall-triggered lahars at Volcán de Colima, Mexico: surface hydro-repellency as initiation process. *Journal of Volcanology and Geothermal Research*, 189(1-2), 105–117. DOI: 10.1016/j.jvolgeores.2009.10.014
- Capra, L., Macías, J. L., Cortés, A., Dávila, N., Saucedo, R., Osorio-Ocampo, S., Arce, J. L., Gavilanes-Ruiz, J. C., Corona-Chávez, P., García-Sánchez, L., Sosa-Ceballos, G., & Vázquez, R. (2016). Preliminary report on the July 10–11, 2015 eruption at Volcán de Colima: Pyroclastic density currents with exceptional runouts and volume. *Journal of Volcanoloy and Geothermal Research*, 310, 39–49. https://doi.org/10.1016/j.jvolgeores.2015.11.022
- Capra, L., Coviello, V., Borselli, L., Márquez-Ramírez, V. H., & Arámbula-Mendoza, R. (2018). Hydrological control of large hurricane-induced

- lahars: evidence from rainfall-runoff modeling, seismic and video monitoring: *Natural Hazards and Earth System Sciences*, 18, 781–794. https://doi.org/10.5194/nhess-18-781-2018
- Church, M., & Jakob, M. (2020). What Is a Debris Flood?. Water Resources Research, 56(8). https://doi.org/10.1029/2020WR027144
- Cole, S. E., Cronin, S. J., Sherburn, S., & Manville, V. (2009). Seismic signals of snow-slurry lahars in motion: 25 September 2007, Mt Ruapehu, New Zealand: Geophysical Reseach Letters, 36(9), L09405. https://doi. org/10.1029/2009GL038030
- Cortes, A., Garduño, V.H., Navarro, C., Komorowski, J.C., Saucedo, R., Macias, J.L., & Gavilanes-Ruiz, J. C. (2005). Carta Geológica del Complejo Volcánico de Colima, Con Geología del Complejo Volcánico de Colima. Cartas Geológicas y Mineras, 10, 0185-4798.
- Cortes, A., Macias, J. L., Capra, L., Garduño-Monroy, V. H. (2010). Sector collapse of the SW flank of Volcán de Colima, México. The 3600 yr BP La Lumbre-Los Ganchos debris avalanche and associated debris flows. *Journal of Volcanology and Geothermal Research*, 197, 52–66. https://doi.org/10.1016/j.jvolgeores.2009.11.013
- Coviello, V., Capra, L., Vázquez, R., & Márquez-Ramírez, V. H. (2018). Seismic characterization of hyperconcentrated flows in a volcanic environment. *Earth Surface Processes*, 43, 2219–2231. https://doi. org/10.1002/esp.4387
- Cronin, S. J., Hodgson, K. A., Neall, V. E., Palmer, A. S., & Lecointre, J. A. (1997). 1995 Ruapehu lahars in relation to the late Holocene lahars of Whangaehu River, New Zealand. New Zealand Journal of Geology and Geophisics, 40, 507–520. DOI: 10.1080/00288306.1997.9514780
- Davila, N., Capra, L., Gavilanes, J. C., Varley, N., & Norini, G. (2007). Recent lahars at Volcán de Colima (Mexico): drainage variation and spectral classification. *Journal of Volcanology and Geothermal Research*, 165, 127–141. https://doi.org/10.1016/j.jvolgeores.2007.05.016
- de Bélizal, E., Lavigne, F., Hadmoko, D. S., Degai, J. P., Dipayana, G. A., Mutagin, B. W., Marfai, M. A., Coquet, M., Le Mauff, B., Robin, A.

- K., Vidal, C., Cholik, N., & Aisyah, N. (2013). Rain-triggered lahars following the 2010 eruption of Merapi volcano, Indonesia: A major risk. *Journal of Volcanology and Geothermal Research*, 261, 330–347. https://doi.org/10.1016/j.jvolgeores.2013.01.010
- Doyle, E. E., Cronin, S. J., Cole, S. E. & Thouret, J.-C. (2010). The coalescence and organization of lahars at Semeru volcano, Indonesia. *Bulletin of Volcanology*, 72, 961–970.
- Doyle, E. E., Cronin, S. J., & Thouret, J. C. (2011). Defining conditions for bulking and debulking in lahars. *Geological Society of America Bulletin*, 123(7/8), 1234–1246. https://doi.org/10.1130/B30227.1
- Dumaisnil, C., Thouret, J. C., Chambon, G., Doyle, E. E., & Cronin, S. J. (2010). Hydraulic, physical and rheological characteristics of rain-triggered lahars at Semeru volcano, Indonesia. *Earth and Surface Processes and Landform*, 35, 1573–1590. https://doi.org/10.1002/esp.2003
- Fagents, S. A., & Baloga, S. M. (2006). Toward a model for the bulking and debulking of lahars. *Journal of Geophysical Research*, 111, B10201. DOI:10.1029/2005JB003986
- Gran, K. B., & Montgomery, D. R. (2005). Spatial and temporal patterns in fluvial recovery following volcanic eruptions: channel response to basin-wide sediment loading at Mount Pinatubo, Philippines. *Geological Society of America Bulletin*, 117(1-2), 195–211. https://doi. org/10.1130/B25528.1
- Hutchinson, J. N. (1988). General report: morphological and geotechnical parameters of landslides in relation to geology and hydrogeology. Proceedings Fifth International Symposium on Landslide (Ed. Bonnard, C.) Rotterdam, Balkema, 1, 3-35.
- Lavigne, F., Thouret, J. C., Voight, B., Suwa, H., & Sumaryono, A. (2000).
 Lahars at Merapi volcano, Central Java: an overview. *Journal of Volcanology and Geothermal Research*, 100, 423–456. https://doi.org/10.1016/S0377-0273(00)00150-5
- Lavigne, F., & Thouret, J. C. (2002). Sediment transport and deposition by rain-triggered lahars at Merapi Volcano, Central Java, Indonesia. Geomophology, 49, 45–69. https://doi.org/10.1016/S0169-555X(02)00160-5
- Manville, V., Németh, K., & Kano, K. (2009) Source to sink: A review of three decades of progress in the understanding of volcaniclastic processes, deposits, and hazards. *Sedimentary Geology*, 220, 136–161. https://doi.org/10.1016/j.sedgeo.2009.04.022
- Márquez-Ramirez, V. H., Capra, L., Martínez-Valdés, J. I., Barroso-Fernández, R., Arámbula-Mendoza, R., González Amezcua, M., & García Flores, R. (2025). Seismic classification of rainfall-induced lahars at Volcán de Colima, México: frequency content as an indicator of sediment concentration. *Journal of South American Earth Sciences*, 167, 105768. https://doi.org/10.1016/j.jsames.2025.105768
- Martínez-Valdés, J. I., Márquez-Ramírez, V. H., Coviello, V., & Capra, L. (2023). Hurricane-induced lahars at Volcán de Colima (México): seismic characterization and numerical modelling. Revista Mexicana de Ciencisas Geológicas, 40(1), 59–70. https://doi.org/10.22201/cgeo.20072902e.2023.1.1709
- Okano, K., Suwa, H. & Kanno, T. (2012). Characterization of debris flows by rainstorm condition at a torrent on the Mount Yakedake volcano, Japan. Geomorphology 136, 88–94.
- Roverato, M., Capra, L., Sulpizio, R., & Norini, G. (2011). Stratigraphic reconstruction of two debris avalanche deposits at Colima Volcano (Mexico): Insights into pre-failure conditions and climate influence. *Journal of Volcanology and Geothermal Research*, 207, 33–46. https://doi.org/10.1016/j.jvolgeores.2011.07.003

- Sarocchi, D., Sulpizio, R., Macias, J. L., & Saucedo, R. (2011). The 17 July 1999 block-and-ash flow (BAF) at Colima Volcano: New insights on volcanic granular flows from textural analysis. *Journal of Volcanology* and Geothermal Research, 204(1-4), 40–56. https://doi.org/10.1016/j. jvolgeores.2011.04.013
- Saucedo, R., Macias, J. L., Sarocchi, D., Bursik, M. I., & Rupp, B. (2008). The rain-triggered Atenquique volcaniclastic debris flow of October 16, 1955 at Nevado de Colima Volcano, Mexico. *Journal of Volcanology* and Geothermal Research, 132, 69–83. https://doi.org/10.1016/j. jvolgeores.2007.12.045
- Scott, K. M., Vallance, J. V., Kerle, N., Macias, J. L., Strauch, W., & Devoli, G. (2005). Catastrophic precipitation-triggered lahars at Casita Volcano, Nicaragua: occurrence, bulking and transformation. *Earth Surface Processes and Landforms*, 30, 59–79. https://doi.org/10.1002/esp.1127
- Sheridan, M. F., Connor, C. B., Connor, L., Stinton, A. J., Galacia, O., & Barrios, G. (2007). October 2005 Debris Flows at Panabaj, Guatemala: Hazard Assessment. American Geophysical Union, Spring Meeting 2007, abstract #V33A-07.
- Tang, H., McGuire, L. A., Kean, J. W., & Smith, J. B. (2020). The Impact of Sediment Supply on the Initiation and Magnitude of Runoff-Generated Debris Flows. *Geophysical Research Letters*, 47(14), e2020GL087643. https://doi.org/10.1029/2020GL087643
- Thouret, J.-C., Antoine, S., Magill, C., & Ollier, C. (2019). Lahars and debris flows: characteristics and impacts. *Earth-Science Reviews*, 201, 103003. https://doi.org/10.1016/j.earscirev.2019.103003
- Umbal, J. V., & Rodolfo, K. S. (1996). The 1991 lahars of southwestern Mount Pinatubo and evolution of the lahar-dammed Mapanuepe lake. In P. I. o. V. a. Seismology (ed), Fire and mud; eruptions and lahars of Mount Pinatubo, 951–970.
- Van Wyk Vries, B., Kerle, N., & Petley, D. (2000). Sector collapse forming at Casita volcano, Nicaragua. *Geology*, 28(2), 167–170.
- Vázquez, R., Capra, L., Caballero-García, L., Arambula, R., & Reyes-Dávila, G. (2014). The Anatomy of a lahar: deciphering the September 15th lahar at Volcán de Colima, Mexico. *Journal of Volcanology and Geothermal Research*, 272, 126–136. https://doi.org/10.1016/j.jvolgeores.2013.11.013
- Vázquez, R., Suriñach, E., Capra, L., Arámbula-Mendoza, R., & Reyes-Dávila, G. (2016a). Seismic characterisation of lahars at Volcán de Colima, Mexico. Bulletin of Volcanology, 78, 8. https://doi.org/10.1007/s00445-016-1004-9
- Vázquez, R., Capra, L., & Coviello, V. (2016b). Factors controlling erosion/ deposition phenomena related to lahars at Volcán de Colima, Mexico. Natural Hazard and Earth System Sciences, 168(8), 1881–1895. https:// doi.org/10.5194/nhess-16-1881-2016
- Zobin, V. M., Placencia, I., Reyes, G., & Navarro, C. (2009). The characteristics of seismic signal produced by lahars and pyroclastic flows: Volcán de Colima, Mexico. *Journal of Volcanology and Geothermal Research*, 179(1-2), 157–167. https://doi.org/10.1016/j.jvolgeores.2008.11.001